

## Catalytic Reforming of Biogas to Produce Environmentally Friendly High Effective Fuels

Tolkyn S. Baizhumanova<sup>a,b,\*</sup>, Manapkhan Zhumabek<sup>a</sup>, Gulnar N. Kaumenova<sup>a</sup>, Svetlana A. Tungatarova<sup>a,b</sup>, Nazgul Talasbayeva<sup>b</sup>, Magira Zhylykybek<sup>b</sup>, Xuliang Zhang<sup>c</sup>, Galina Xanthopoulou<sup>d</sup>, Aissana Y. Tolembek<sup>e</sup>

<sup>a</sup>D.V. Sokolsky Institute of Fuel, Catalysis and Electrochemistry, 142 Kunaev str., Almaty, 050010, Kazakhstan

<sup>b</sup>Al-Farabi Kazakh National University, 71, al-Farabi str., Almaty, 050040, Kazakhstan

<sup>c</sup>Pingdingshan University, Pingdingshan, Henan, 467000, China

<sup>d</sup>Institute of Nanoscience and Nanotechnology, NCSR Demokritos, Athens, 15310, Greece

<sup>e</sup>Nazarbayev Intellectual School, 195, Ataturic str., Turkestan, Kazakhstan

t.baizhumanova@ifce.kz

In today's world, environmental issues are becoming more and more relevant. In connection with the growing industrial activity of mankind, a large amount of CH<sub>4</sub> and CO<sub>2</sub> is emitted into the atmosphere. Since the start of the Industrial Revolution, CO<sub>2</sub> concentrations have increased by more than 45 %, from 280 ppm in the mid-18<sup>th</sup> century to 415 ppm in 2019. Biogas mainly consists of 50 - 87 % methane, 13 - 50 % carbon dioxide and other gases. Conversion of biogas solves two important issues related to the utilization of greenhouse gases and the possibility of obtaining synthesis-gas with an optimal ratio of 1 : 1. Carrying out the Fischer-Tropsch synthesis reaction, the production of gasoline, jet fuel, ethanol and other oxygen-containing compounds is possible at this ratio. Development of new applied catalysts, as well as optimal technological conditions for synthesis-gas production in the process of catalytic conversion of biogas, is a contribution to the petrochemical sector, namely gas processing. Optimal conditions for the oxidative conversion of a model mixture of biogas into synthesis-gas on Ni-, Co- monometallic and Ni-Co bimetallic catalysts at different ratios to obtain maximum yield of products with rational consumption of raw materials and energy were determined: T = 700 °C, GHSV = 6,000 h<sup>-1</sup>, CH<sub>4</sub> : CO<sub>2</sub> : Ar = 1 : 1 : 1 ratio in the reaction mixture.

### 1. Introduction

Vast reserves of gaseous hydrocarbons and gas mixtures containing them, primarily natural gas and methane as its main component, make them a promising resource that can meet the needs of mankind in energy and hydrocarbon raw materials. One of the serious problems of modern gas chemistry remains the high costs of hydrocarbon processing into synthesis-gas, which is the main intermediate product of their transformation into final chemical products and liquid fuel. The search for more efficient and economical (in comparison with steam and autothermal reforming of natural gas) technologies for production of synthesis-gas is becoming one of the main scientific and technical directions in energy and gas chemistry.

Despite significant reserves of natural and shale gas, direct synthesis of chemicals using methane as a raw material in the chemical industry is still a huge problem. Methane conversion is divided into two types: direct and indirect conversion (Holmen et al., 2009). Direct conversion mainly involves direct oxidation of methane to methanol (Raja et al., 1997) and formaldehyde (Herman et al., 1997), the combination of methane oxidation to ethylene and ethane (Pak et al., 1998) and production of aromatic hydrocarbons (Guo et al., 2014). Methane is converted into synthesis-gas (Tungatarova et al., 2021), and then various chemical products or liquid fuels are produced from it through the Fischer-Tropsch reaction (Kang et al., 2017) at the indirect methane conversion.

Over the past 30 years, research on the reaction of biogas to synthesis-gas has made some progress, mainly related to the development and design of catalysts and reactors, reduction of coke formation, elucidation of

the mechanism and kinetics of the reaction, etc. Although the conversion of biogas to synthesis-gas has great environmental and economic benefits, it has not yet been applied on an industrial scale due to technological problems that need to be solved. Conversion of biogas into synthesis-gas mainly occurs at very high temperatures, during which carbon is easily formed. The formation, migration and agglomeration of active metal particles lead to rapid deactivation of the catalyst. A lot of research on the process of biogas conversion to synthesis-gas is mainly focused on solving the problem of rapid catalyst deactivation. Development of a catalyst with a high degree of conversion, long service life and prevention of sintering and carbon deposition is an important problem that has not yet been solved.

Supported metal catalysts are mainly used in the production of synthesis-gas by dry methane reforming. Noble metals of the VIII group: Rh (Boukha et al., 2018), Ru (Rabe et al., 2007), Pt (Khajenoori et al., 2013) and Pt-Ru bimetallic compositions (Tungatarova et al., 2019) are the active components of the catalyst. Studies have shown that noble metals have a high conversion rate and structural advantages in biogas to synthesis-gas conversion reactions. Therefore, they are very suitable as active components of the reaction catalyst. However, the cost of precious metals limits their large-scale use.

Non-noble metal catalysts are widely used as an active component in methane reforming reactions, such as Ni (Marinho et al., 2019), Fe (Tsoukalou et al., 2016), and Co-Ni (Turap et al., 2020). Non-noble metal catalysts may have catalytic activity close to that of noble metals. There are large reserves of them in nature, and they have a relatively low cost, which makes their use more promising.

Active and thermally stable supported Ni- and Co-monometallic, as well as Ni-Co bimetallic catalysts, selectively leading the process of biogas conversion into synthesis-gas, were synthesized.

## 2. Experimental

The catalysts were obtained by the traditional method of air impregnation by moisture capacity. The alumina was first dried at 110°C. Then the moisture content in the carrier was determined. Titrated Ni- and Co-solutions were prepared with a concentration of 0.15 g/mL from nitrate salts of  $\text{Ni}(\text{NO}_3)_6 \cdot 6\text{H}_2\text{O}$  and  $\text{Co}(\text{NO}_3)_6 \cdot 6\text{H}_2\text{O}$ . A certain amount of a titrated solution of Ni, Co or a mixture thereof is injected into a porcelain cup, depending on the percentage of metals in the catalysts. Then a certain amount of distilled water is added. The whole mixture is well mixed and a dried carrier is poured into the solution. The resulting catalyst was stirred in air and dried at 250°C for 1 h, then calcined at 500°C for 2 h. The following catalysts were prepared: 10%Ni/ $\theta$ - $\text{Al}_2\text{O}_3$ , 9%Ni-1%Co/ $\theta$ - $\text{Al}_2\text{O}_3$ , 7%Ni-3%Co/ $\theta$ - $\text{Al}_2\text{O}_3$ , 5%Ni-5%Co/ $\theta$ - $\text{Al}_2\text{O}_3$ , 3%Ni-7%Co/ $\theta$ - $\text{Al}_2\text{O}_3$ , 1%Ni-9%Co/ $\theta$ - $\text{Al}_2\text{O}_3$ , 10% Co/ $\theta$ - $\text{Al}_2\text{O}_3$ .

Analysis of the initial mixture and the reaction products was performed using "Chromos GC-1000" chromatograph, which was equipped with packed and capillary columns. The packed column was used for the analysis of  $\text{H}_2$ ,  $\text{O}_2$ ,  $\text{N}_2$ ,  $\text{CH}_4$ ,  $\text{C}_2\text{H}_6$ ,  $\text{C}_2\text{H}_4$ ,  $\text{C}_3$ - $\text{C}_4$  hydrocarbons, CO and  $\text{CO}_2$ . A capillary column was used to analyze of liquid organic substances, such as alcohols, acids, aldehydes, ketones and aromatic hydrocarbons. Temperature of the detector by thermal conductivity – 200°C, evaporator temperature – 280°C, column temperature – 40°C. The speed of the Ar as carrier gas was 10 mL/min. The chromatographic peaks were calculated from the calibration curves plotted for the respective products using the "Chromos" software for pure substances. Based on the measured areas of the peaks corresponding to the amount of the introduced substance, a calibration curve  $V = f(S)$  was constructed, where V - amount of substance in mL, S - peak area in  $\text{cm}^2$ . Concentrations of the obtained products were determined on the basis of the obtained calibration curves. The error of chromatographic measurements is 2-3 %. The balance by products was  $\pm 3.0\%$ .

The morphology of nanostructured carbon supported on the surface of catalyst was analyzed using a transmission electron microscope JEM-1400 Plus (Japan). The TEM images were recorded at an accelerating voltage of 120 kV. Before the analysis, ultrasonic dispersion of the catalyst samples was carried out in ethanol at room temperature. A few drops of a sample of a catalyst containing a suspension were placed on a carbon-coated copper grid. The copper mesh was then used for visualization for each sample. Physico-chemical studies were carried out in the Laboratory of Industrial Chemistry of the University of Abo Akademi (Turku, Finland). The resulting catalysts were characterized by X-ray diffraction (XRD) using  $\text{CuK}\alpha_1$  radiation on a Siemens Spellman DF3 spectrometer with 10% KCl as an internal standard for semi-quantitative XRD analysis. Specific surface area determination was done by nitrogen physisorption at 350 °C on a GAPP V-Sorb 2,800 Analyser using helium as a carrier gas.

The catalysts were tested in a quartz reactor with a fixed layer with a diameter of 10 mm and a length of 40 cm at atmospheric pressure. The catalyst (2 mL) was placed between quartz granules in a tubular reactor.

### 3. Results and discussion

It was found that TEM images of spent 5%Ni-5%Co/ $\theta$ -Al<sub>2</sub>O<sub>3</sub> and 7%Ni-3%Co/ $\theta$ -Al<sub>2</sub>O<sub>3</sub> catalysts after operation show the formation of carbon nanotubes with a diameter from 10 to 30 nm (Figure 1).

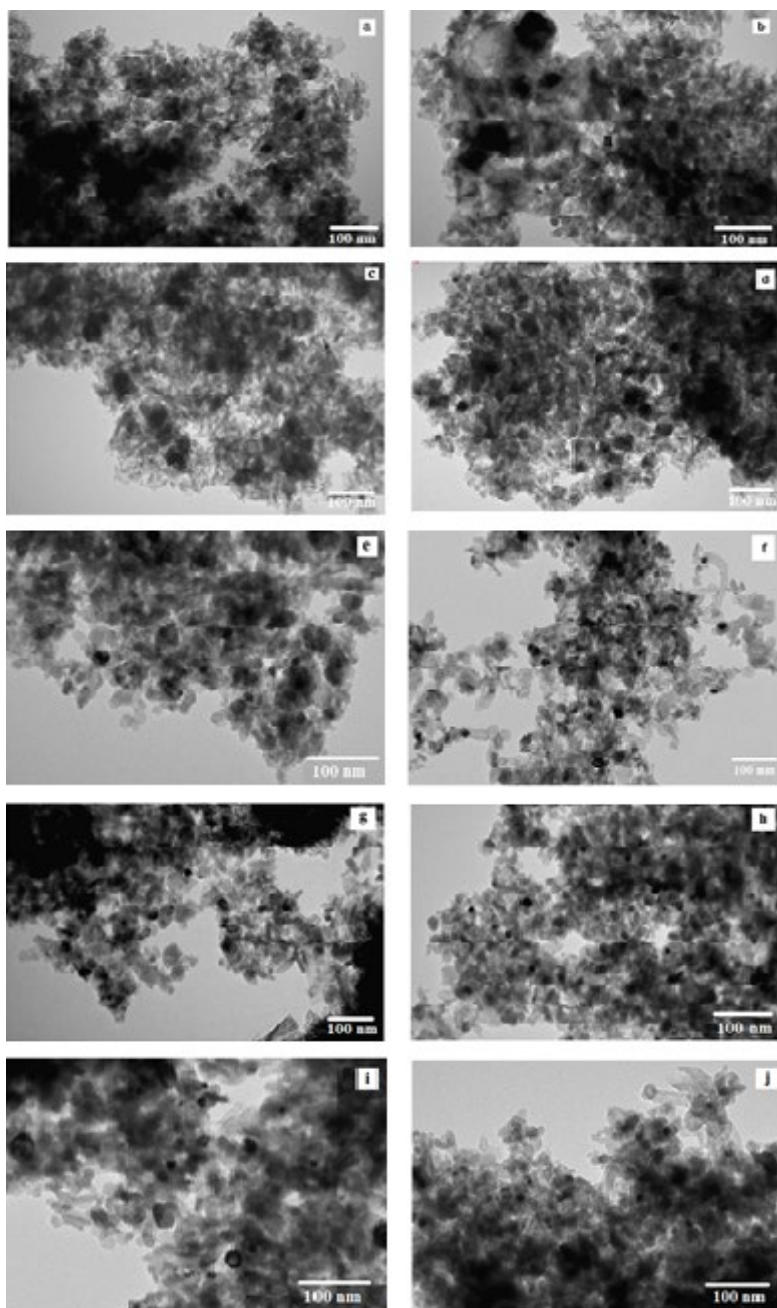


Figure 1: TEM images of a) fresh and b) spent 10%Co/ $\theta$ -Al<sub>2</sub>O<sub>3</sub>, c) fresh and d) spent 1%Ni-9%Co/ $\theta$ -Al<sub>2</sub>O<sub>3</sub>, e) fresh and f) spent 5%Ni-5%Co/ $\theta$ -Al<sub>2</sub>O<sub>3</sub>, g) fresh and h) spent 9%Ni-1%Co/ $\theta$ -Al<sub>2</sub>O<sub>3</sub> and i) fresh and j) spent 10%Ni/ $\theta$ -Al<sub>2</sub>O<sub>3</sub>

An uneven distribution of various elements can be observed in Figure 1. As a rule, one of the reasons for deactivation of catalyst may be deposition of carbon in pores of catalyst (Kim et al., 2000). Nickel-cobalt catalysts supported on  $\theta$ -Al<sub>2</sub>O<sub>3</sub> have large pores (16 - 18 nm), which contributes to their stability. From the TEM images, it can be seen that the metal oxide particles were in the range of 10 - 25 nm without much difference between fresh and spent catalysts. The formation of carbon nanotubes in the current case of methane reforming corresponds to the data obtained in (Zhang et al., 2020), where it was reported that

graphite carbon filamentous crystals can be formed under dry methane conditions at 700 - 850 °C on a nickel catalyst. It was also reported in (Zhang et al., 2020) that graphite carbon whiskers have same diameter as metal crystals. In addition, methane cracking is one of the reasons for the formation of coke over Ni/ $\gamma$ -Al<sub>2</sub>O<sub>3</sub> (Zhang et al., 2020). Coking of bimetallic 5% Ni - 10% Co/ $\gamma$ -Al<sub>2</sub>O<sub>3</sub> catalysts was also observed during dry reforming of methane at 700 °C (Kassymkan et al., 2020).

The amounts of Co and Ni in the spinel exceeded their nominal loading (Table 1). It should, however, be noted that the peak at ca. 20° can be assigned also to other structures, such as (Co<sub>0.87</sub>Al<sub>0.13</sub>), ((Al<sub>0.60</sub>Co<sub>0.40</sub>)<sub>2</sub>O<sub>4</sub>) (Casado et al., 1984). In this case, the corrected amounts of Co and Ni are corresponding to their rated load. In the fresh catalysts, Co and Ni are present in the form of Co<sub>3</sub>O<sub>4</sub>, NiO (Sasaki et al., 1979) and as Co<sub>3-x</sub>Ni<sub>x</sub>O<sub>4</sub> and Ni<sub>1-x</sub>Co<sub>x</sub>O, while in the spent catalyst also metal phase was present (Table 1) (Takanabe et al., 2005).

Table 1: XRD and TEM results

Catalysts	Fraction of phases, %				Crystal size, nm (XRD)			Crystal size, nm (TEM)
	$\alpha$ -Al <sub>2</sub> O <sub>3</sub>	Co <sub>3-x</sub> Ni <sub>x</sub> O <sub>4</sub>	Ni <sub>1-x</sub> Co <sub>x</sub> O	Co <sub>1-x</sub> Ni <sub>x</sub>	D <sub>Co<sub>3-x</sub>Ni<sub>x</sub>O<sub>4</sub></sub>	D <sub>Ni<sub>1-x</sub>Co<sub>x</sub>O</sub>	D <sub>Co<sub>1-x</sub>Ni<sub>x</sub></sub>	
10%Co/ $\theta$ -Al <sub>2</sub> O <sub>3</sub>	<1	20.3	<1	<1	18	n.d.	(20)	14(17)
1%Ni-9%Co/ $\theta$ -Al <sub>2</sub> O <sub>3</sub>	<1	19.2	<1	<1	16	n.d.	(18)	39(28)
5%Ni-5%Co/ $\theta$ -Al <sub>2</sub> O <sub>3</sub>	2.1	16.5	1.2	<1	13	<sup>a</sup>	(14)	22(17)
9%Ni-1%Co/ $\theta$ -Al <sub>2</sub> O <sub>3</sub>	1.6	<1	7.1	<1	<sup>a</sup>	17	(13)	21(17)
10%Ni/ $\theta$ -Al <sub>2</sub> O <sub>3</sub>	2.9	<1	6.8	<1	<sup>a</sup>	16	(12)	17(16)

<sup>a</sup> below the detection limit

Spent catalysts are indicated in parentheses

The spinel structure is found in all other samples but not in 9% Ni-1% Co/ $\theta$ -Al<sub>2</sub>O<sub>3</sub> and 10% Ni/ $\theta$ -Al<sub>2</sub>O<sub>3</sub> since only Ni cannot form a spinel structure. The amount of Co is insufficient to stabilize the spinel structure in Ni-rich catalysts. Spinel structure formation is preferred for cobalt oxide due to coexistence of Co<sup>2+</sup> and Co<sup>3+</sup>. The unit cell sizes of  $\theta$ -Al<sub>2</sub>O<sub>3</sub> and  $\alpha$ -Al<sub>2</sub>O<sub>3</sub> phases agree with the corresponding literature values (Feret et al., 2000). The crystal sizes of the particles were determined from the individual peak widths using the Scherrer formula. The chosen peaks were (202/002), (200), (440), (200) and (002) for  $\theta$ -Al<sub>2</sub>O<sub>3</sub>, Ni<sub>1-x</sub>Co<sub>x</sub>O, Co<sub>3-x</sub>Ni<sub>x</sub>O<sub>4</sub>, Co<sub>1-x</sub>Ni<sub>x</sub> and graphite, respectively. Large crystal particle sizes of the spinel structure were observed in the fresh 10% Co/ $\theta$ -Al<sub>2</sub>O<sub>3</sub>, 9% Ni-1% Co/ $\theta$ -Al<sub>2</sub>O<sub>3</sub> and 10% Ni/ $\theta$ -Al<sub>2</sub>O<sub>3</sub> catalysts (Table 1). The metal particle size in the spent catalysts decreased with increasing nickel content most probably due to easier reduction of nickel in comparison to cobalt (Al-Fatesh et al., 2019). Furthermore, the smallest Co<sub>3-x</sub>Ni<sub>x</sub>O<sub>4</sub> particles were found in 5% Ni-5% Co/ $\theta$ -Al<sub>2</sub>O<sub>3</sub> catalysts, which exhibited the same amount of  $\alpha$ -Al<sub>2</sub>O<sub>3</sub> as 10% Co/ $\theta$ -Al<sub>2</sub>O<sub>3</sub>. On the other hand, the same metal oxide particle size as for 10% Co/ $\theta$ -Al<sub>2</sub>O<sub>3</sub> catalyst was found for 10% Ni/ $\theta$ -Al<sub>2</sub>O<sub>3</sub> catalyst with a higher amount of  $\alpha$ -Al<sub>2</sub>O<sub>3</sub>. This indicates that the amount of  $\alpha$ -Al<sub>2</sub>O<sub>3</sub> did not have any major effect on metal oxide particle size. The spent catalysts with nickel content between 5-10 wt% contained additionally crystalline graphite with the size of 4-6 nm. The crystal sizes of  $\theta$ -Al<sub>2</sub>O<sub>3</sub> were the same for different catalysts decreasing slightly for the spent catalysts.

The variation of reaction space velocity and temperature, where the conversion of CH<sub>4</sub> and CO<sub>2</sub> increases with increasing of space velocity were investigated. It reaches the maximum at 6,000 h<sup>-1</sup> and T = 700 °C. Then the conversion of CH<sub>4</sub> decreased from 97.3% to 93.0%, and CO<sub>2</sub> conversion decreased from 93.0% to 87.0%. Thus, it was determined that 6,000 h<sup>-1</sup> and T = 700 °C are optimal for conversion of CH<sub>4</sub> and CO<sub>2</sub> into synthesis-gas (Zhang et al., 2020).

The characteristics of Ni-, Co-monometallic and Ni-Co bimetallic samples supported on  $\theta$ -Al<sub>2</sub>O<sub>3</sub> were studied for reforming CH<sub>4</sub> with CO<sub>2</sub> at 700 °C. Methane conversion was maximal for 5%Ni-5%Co/ $\theta$ -Al<sub>2</sub>O<sub>3</sub> and 3%Ni-7%Ni/ $\theta$ -Al<sub>2</sub>O<sub>3</sub> catalysts after 2 h of operation. The degree of decontamination calculated on the base of methane conversion was the highest for 5%Ni-5%Co/ $\theta$ -Al<sub>2</sub>O<sub>3</sub>, and the lowest for 10%Co/ $\theta$ -Al<sub>2</sub>O<sub>3</sub> catalysts. The highest conversion of methane was obtained on monometallic catalysts, although the carbon content in 10%Co/ $\theta$ -Al<sub>2</sub>O<sub>3</sub> catalyst was much lower than in 10%Ni/ $\theta$ -Al<sub>2</sub>O<sub>3</sub> catalyst.

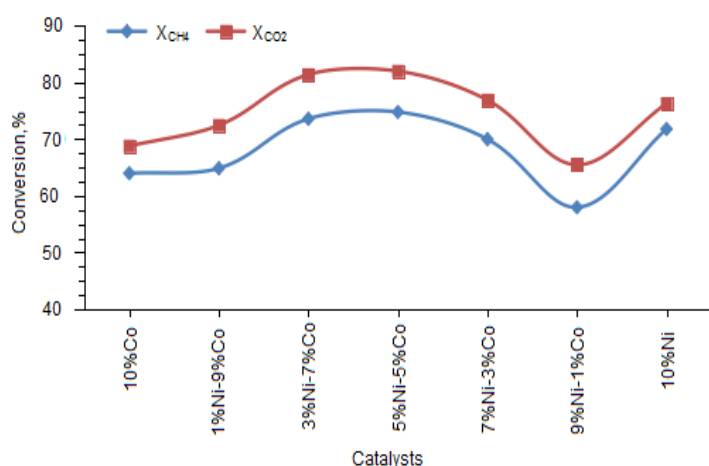


Figure 2: Comparison of the conversion of methane and carbon dioxide on a series of developed Ni-, Co- and Ni-Co catalysts at 700 °C, CH<sub>4</sub>: CO<sub>2</sub>: Ar=1:1:1 and space velocity of gases 6,000 h<sup>-1</sup>

The optimal conditions for oxidative conversion reaction of a model mixture of biogas into synthesis-gas were determined: T = 700 °C, GHSV = 6,000 h<sup>-1</sup>, the ratio of gases in the reaction mixture CH<sub>4</sub> : CO<sub>2</sub> : Ar = 1:1:1 and the ratio of active elements Ni:Co = 1 : 1 to obtain the maximum yield of products with rational consumption of raw materials and energy. A new Ni<sub>1-x</sub>Co<sub>x</sub>O phase appeared in the nickel-cobalt catalyst, which is assumed to have led to high activity and stability of the catalyst (Tran et al., 2020).

#### 4. Conclusions

New oxide catalysts have been prepared by the traditional method of impregnation by moisture capacity, showing high activity in the catalytic conversion of biogas into synthesis gas. It was found that 5% Ni - 5% Co/θ-Al<sub>2</sub>O<sub>3</sub> catalyst has high initial activity among bimetallic compounds. CH<sub>4</sub> and CO<sub>2</sub> conversion were 75 and 82% at 700 °C, accordingly. However, the activity decreased rapidly with increasing time, according to the XRD data, and along with the phase transition of spinel-type metal oxide into the structure of a mixed metal of a Co - Ni face-centered cubic type. Synthesis-gas with the ratio of H<sub>2</sub> / CO = 1 / 1 was obtained, which is most suitable for its further use in the synthesis of methanol and hydrocarbons by the Fischer-Tropsch mechanism.

#### Nomenclature

D – diameter, nm

GHSV – gas hourly space velocity, h<sup>-1</sup>

S - peak area, cm<sup>2</sup>

T – temperature, °C

V - amount of substance, mL

#### Acknowledgments

The work was supported by the Ministry of Education and Science of the Republic of Kazakhstan (AP08052090).

#### References

- Al Fatesh A.S., Abu-Dahrieh J.K., Atia H., Armbruster U., Ibrahim A.A., Khan W.U., Fakeeha A.H., 2019, Effect of pre-treatment and calcination temperature on Al<sub>2</sub>O<sub>3</sub>-ZrO<sub>2</sub> supported Ni-Co catalysts for dry reforming of methane, *International Journal of Hydrogen Energy*, 44, 21546–21558.
- Boukha Z., Jiménez González C., de Rivas B., GonzálezVelasco J.R., Gutiérrez Ortiz J.I., López Fonseca R., 2014, Synthesis, characterisation and performance evaluation of spinel-derived Ni/Al<sub>2</sub>O<sub>3</sub> catalysts for various methane reforming reactions, *Applied Catalysis B: Environmental*, 158–159, 190–201.
- Casado P.G., Rasines I., 1984, The series of spinels Co<sub>3-s</sub>Al<sub>s</sub>O<sub>4</sub> (0 < s < 2): study of Co<sub>2</sub>AlO<sub>4</sub>, *Journal of Solid State Chemistry*, 52, 187–190.
- Feret F.R., Roy D., Boulanger C., 2000, Determination of alpha and beta alumina in ceramic alumina by X-ray diffraction, *Spectrochimica Acta Part B: Atomic Spectroscopy*, 55, 1051–1061.
- Guo X., Fang G., Li G., Ma H., Fan H., Yu L., Bao X., 2014, Direct, nonoxidative conversion of methane to ethylene, aromatics, and hydrogen, *Science*, 344(6184), 616–619.

- Herman R.G., Sun Q., Shi C., Klier K., Wang C.-B., Hu H., Wachs L.E., Bhasin M.M., 1997, Development of active oxide catalysts for the direct oxidation of methane to formaldehyde, *Catalysis Today*, 37(1), 1–14.
- Holmen A., 2009, Direct conversion of methane to fuels and chemicals, *Catalysis Today*, 142(1–2), 2–8.
- Kang D., Lim H.S., Lee J.W., 2017, Enhanced catalytic activity of methane dry reforming by the confinement of Ni nanoparticles into mesoporous silica, *International journal of Hydrogen energy*, 42(16), 11270–11282.
- Kassymkan K., Zhang X., Sarsenova R.O., Zheksenbaeva Z.T., Tungatarova S.A., Baizhumanova T.S., 2020, Catalytic processing of natural gas into olefins, *Chemical Engineering Transactions*, 81, 1057–1062.
- Khajenoori M., Rezaei M., Nematollahi B., 2013, Preparation of noble metal nanocatalysts and their applications in catalytic partial oxidation of methane, *Journal of Industrial and Engineering Chemistry*, 19(3), 981–986.
- Kim J.H., Suh D.J., Park T.J., Kim K.L., 2000, Effect of metal particle size on coking during CO<sub>2</sub> reforming of CH<sub>4</sub> over Ni–alumina aerogel catalysts, *Applied Catalysis A: General*, 197(2), 191–200.
- Marinho A.L.A., Rabelo-Neto R.C., Epron F., Bion N., Toniolo F.S., Noronha F.B., 2019, Embedded Ni nanoparticles in CeZrO<sub>2</sub> as stable catalyst for dry reforming of methane, *Applied Catalysis B: Environmental*, 268, 118387.
- Pak S., Qiu P., Lunsford J.H., 1998, Elementary reactions in the oxidative coupling of methane over Mn/Na<sub>2</sub>WO<sub>4</sub>/SiO<sub>2</sub> and Mn/Na<sub>2</sub>WO<sub>4</sub>/MgO catalysts, *Journal of Catalysis*, 179(1), 222–230.
- Rabe S., Nachtegaal M., Vogel F., 2007, Catalytic partial oxidation of methane to synthesis gas over a ruthenium catalyst: the role of the oxidation state, *Physical Chemistry Chemical Physics*, 9, 1461–1468.
- Raja R., Ratnasamy P., 1997, Direct conversion of methane to methanol, *Applied Catalysis A: General*, 158(1–2), L7–L15.
- Sasaki S., Fujino K., Takeuchi Y., 1979, X-ray determination of electron-density distributions in oxides, MgO, MnO, CoO, and NiO, and atomic scattering factors of their constituent atoms, *Proceedings of the Japan Academy. Series B*, 55, 43–48.
- Takanabe K., Nagaoka K., Nariai K., Aika K.I., 2005, Titania-supported cobalt and nickel bimetallic catalysts for carbon dioxide reforming of methane, *Journal of Catalysis*, 232, 268–275.
- Tran N.T., Van Le Q., Van Cuong N., Nguyen T.D., Phuc N.H.H., Phuong P.T.T., Monir M.U., Aziz A.A., Truong Q.D., Abidin S.Z., Nanda S., Vo D.V.N., 2020, La-doped cobalt supported on mesoporous alumina catalysts for improved methane dry reforming and coke mitigation, *Journal of the Energy Institute*, 93(4), 1571–1580.
- Tsoukalou A., Imtiaz Q., Kim S.M., Abdala P.M., Yoon S., Müller C.R., 2016, Dry-reforming of methane over bimetallic Ni–M/La<sub>2</sub>O<sub>3</sub> (M = Co, Fe): The effect of the rate of La<sub>2</sub>O<sub>2</sub>CO<sub>3</sub> formation and phase stability on the catalytic activity and stability, *Journal of Catalysis*, 343, 208–214.
- Tungatarova S., Xanthopoulou G., Vekinis G., Baizhumanova T., Zhumabek M., Kotov S., Manabayeva A., 2021, Production of hydrogen-containing clear fuel from biogas, *Chemical Engineering Transactions*, 88, 2026–2033.
- Tungatarova S., Baizhumanova T., Zheksenbaeva Z., Zhumabek M., Kaumenova G., Aubakirov Y., Begimova G., 2019, Nanosized composite Pt–Ru catalysts for production of modern modified fuels, *Chemical Engineering & Technology*, 42(4), 918–924.
- Turap Y., Wang I., Fu T., Wu Y., Wang Y., Wang W., 2020, Co–Ni alloy supported on CeO<sub>2</sub> as a bimetallic catalyst for dry reforming of methane, *International Journal of Hydrogen Energy*, 45(11), 6538–6548.
- Zhang X., Zheksenbaeva Z.T., Sarsenova R.O., Tungatarova S.A., Baizhumanova T.S., Zhevnikskiy S.I., 2020, Oxide Ni–Cu catalysts for the purification of exhaust gases, *Chemical Engineering Transactions*, 81, 925–930.
- Zhang X., Maki-Arvela P., Palonen H., Murzin D.Y., Aubakirov Y.A., Tungatarova S.A., Baizhumanova T.S., 2020, Catalytic reforming of methane into synthesis-gas, *Materials Today. Proceedings*, 31, 595–597.